

FTIR Analysis of Particulate Matter Collected on Teflon Filters in Columbus, OH

A Senior Honors Thesis

Presented in Partial Fulfillment of the Requirements for graduation
with distinction in Chemistry in the undergraduate colleges
of The Ohio State University

by

Patrick Veres

The Ohio State University
June 2005

Project Adviser: Professor Heather Allen, Department of Chemistry

Abstract

The chemical characterization of particulate matter (PM) to which humans are exposed to provides information important to the understanding of our chemical environment and associated health risks. In this research, experimental methods have been developed for the collection and qualitative characterization of personal exposure to PM. Three ambient samples have been collected at various locations in Columbus, OH to demonstrate the analytical capabilities of the techniques used. The methods developed will be used in future PM compositional studies and can be extended to include quantitative functional group analysis.

Field samples of PM were collected over a 24-h period on Teflon filters with the Sioutas cascade impactor operated at 9 L/min. PM samples were fractionated into the following size distributions: $> 2.5 \mu\text{m}$, $2.5 - 1.0 \mu\text{m}$, $1.0 - 0.50 \mu\text{m}$, $0.50 - 0.25 \mu\text{m}$, and $< 2.5 \mu\text{m}$. FTIR analysis of the samples provided important details on the functional group composition of the PM samples. A differential washing procedure was used to assess the polarity of particle constituents.

1. Introduction

Particulate matter is a term describing airborne particles and aerosols. PM exists in the atmosphere from either direct emissions of anthropogenic and biogenic sources or as a result of secondary reactions between pollutants. These particles are referred to as primary and secondary particles respectively. Common examples of particulate sources include combustion nuclei, atmospheric dust, and tobacco smoke. Atmospheric particles differ in terms of their number concentration, chemical composition, size, mass, aerodynamic and optical properties. Variation in particle properties is dependant on several conditions including emissions source and regional

atmospheric composition. Of these characteristics, size is often the most important due to their relevance to climate, particle source, and health consequences.

Particle size is measured in terms of diameter; however atmospheric particles are rarely spherical. Therefore, a commonly used metric is aerodynamic diameter (D_a), which is based upon a sphere of unit density (1 g cm^{-3}) with the same terminal falling speed as the particle being considered. Particles exist as either a solid or a liquid with diameters ranging from ~ 0.002 to $\sim 100 \text{ }\mu\text{m}$. $\text{PM}_{2.5}$ refers to particles with an aerodynamic diameter of $< 2.5 \text{ }\mu\text{m}$, these are considered fine particles. Similarly, $\text{PM}_{1.0-2.5}$ represents particles lying between 1 and $2.5 \text{ }\mu\text{m}$ in diameter. Particles with an aerodynamic diameter larger than $2.5 \mu\text{m}$ are classified as coarse particles.

Fine particles comprise the largest number of particles as well as the greatest fraction of total particle mass. $\text{PM}_{2.5}$ represents approximately one-half of the particulate mass in urban areas. Those in the larger end of the size range tend to have low suspension times and rapidly fall out of the atmosphere; these include very fine sand or a fine mist. In terms of atmospheric chemistry and health effects, particulate matter in the range of 10 to $0.002 \text{ }\mu\text{m}$ is the most important as a result of longer residency times and their ability to penetrate deep within the lungs (Finlayson-Pitts and Pitts, 1999).

Determination of particle size distribution in the atmosphere is made difficult due to this concentration of particle density in the fine PM region. A general plot of particle numbers as a function of diameter, D_a , would appear to be a narrow spike at the origin. The resulting graph would provide little detail about coarse fractions due to scaling issues originating from the large number of fine particles. As a result, experimental collection of PM samples characterizes size intervals by a 50% cutoff point. A 50% cutoff point is defined as the diameter of spheres with

unity density of which one-half are collected. The result is collection of particles in a specific range of aerodynamic diameters. In multistage impactors, such as the one used in this experiment, the cutoff point defines each collection stage. This practice fractionates particle intervals unequally based on particle diameter to ensure a more detailed assessment of particle distribution. An example of this concept applied to a four-stage impactor is shown in Table 1.1. The resulting graphical representation of size versus particle number, using 50% cutoff points as a metric, provides a more detailed profile of ambient particle distribution.

Particles having a diameter of 2.5 μm and lower are of greatest concern relative to epidemiological studies. These particles can be deposited in the gas-exchange regions of the respiratory tract where little biological defense is present. It follows that PM concentrations have been heavily monitored as a result of concerns that respirable PM is a risk factor for significant health problems. Recent studies have shown that episodes of high PM levels correlate well with asthma in the elderly and children (Lin et al., 2002), deaths due to cardiovascular health (Hoek et al., 2001), and respiratory deaths (Braga et al., 2001). Thus, it has recently become important to study the chemical composition of various PM size fractions.

The composition of individual particles is highly dependent upon the source of origin. Particulate matter in the atmosphere contains a complex mixture of water-soluble inorganic salts and insoluble mineral dust. Atmospheric particles also contain carbonaceous material consisting of organics ranging from very soluble to insoluble plus elemental carbon. (Jacobson et al., 2000). Ultrafine particles, $\text{PM} < 0.01 \mu\text{m}$, are often a result of homogenous nucleation and tend to contain secondary species such as sulfate and organics. Particles in the range of 0.01 – 0.08 μm result from combustion processes, particle coagulation and condensation of gas-phase reactions. These often contain trace metals characteristic of combustion, carbon, sulfates, nitrates and polar

organics. Course particles $> 2.5 \mu\text{m}$ results from mechanical processes and contain species typical of sea salts, soils, etc. (Pitts and Pitts 1999).

Using FTIR, several studies have observed inorganics such as SO_4^{2-} , NO_3^- , SiO_4^{2-} , and NH_4^+ , and organic functional groups like aliphatic carbons, carbonyls, and organic nitrates (Maria et al., 2002; Marley et al., 1993). The findings of such studies have identified common constituents; yet, PM composition varies with the region from which the particle originated.

In a 2003 study, measurements of $\text{PM}_{10-2.5}$ and $\text{PM}_{2.5}$ gave a distinctly different profile for Beirut, Lebanon than for similar studies conducted in Western Mediterranean cities (Shaka et al., 2004). Thus, it is expected that the PM composition of particulates as measured in Columbus, OH have a unique profile specific to regional conditions. For this reason, inexpensive methods of PM collection and analysis must be developed to perform additional regional monitoring. Measurements of chemically characterized PM exposures will aid investigators in evaluating personal risk of exposure to particles. In return, such studies will provide data relevant to epidemiological assessment of regional exposures and emission sources.

Fourier transform infrared (FTIR) spectroscopy is an ideal nondestructive method for PM chemical analysis. Two methods of qualitative FTIR analysis are predominantly used to analyze particulate samples. Transmission and attenuated total reflectance (ATR) spectroscopy both provide novel techniques for PM compositional studies. Both methods provide detailed information on the composition of the sample being analyzed. ATR spectroscopy, however, has limited applications in quantitative studies since it has a penetration depth of only a few microns. Therefore, for quantitative studies, transmission spectroscopy, which penetrates into the bulk of the substance, is ideal. The qualitative analysis involved in this study allowed for both transmission and ATR spectroscopic techniques to be explored as potential analytical tools.

FTIR transmission spectroscopy of PM samples on Teflon filters can be adapted to both qualitative and quantitative analyses. The process involves monitoring the absorption of an infrared beam that is passed directly through the sample and filter. The difference in intensity of the initial infrared beam (i.e. the absorbance of the sample) can be used to identify the chemical composition of the PM collected. The resulting absorption bands are unique to specific functional groups and are proportional to the amount of sample present. This method of measurement, as opposed to ATR, measures species both within the bulk of the sample and at the surface. Therewith, a functional group analysis can be performed to give quantitative and qualitative information.

Several groups have studied ATR spectroscopy as it relates to particulate matter analysis (Shaka et al. 2004). In an ATR experiment the infrared beam is concentrated across the surface of the sample only a few μm in depth. A simplified diagram of a typical ATR instrument is shown in Figure 1.2. A sample is placed on a transparent crystalline material with a high refractive index through which is passed the IR beam. As the IR wave undergoes complete internal reflection, a small amount of radiation enters the sample medium. The radiation that enters the sample is known as an evanescent wave and is absorbed at certain wavelengths, or absorption bands, characteristic of components within the sample. The amount of absorption at various wavelengths can be translated to describe the chemical composition of the sample.

In this study, multiple techniques were investigated to determine the most efficient methods for PM collection and analysis. Ambient samples were qualitatively analyzed using FTIR spectroscopy to identify a variety of inorganics and organic functional groups such as NH_3^+ , SiO_4^{2-} , and aliphatic carbons. The groups identified were selected due to their commonality to atmospheric PM and the availability of data from similar studies (Maria et al.,

2003, Blando et al., 1998). This work presents a qualitative analysis of the protocol developed for this particular investigation. The analysis provides insight into the advantages and disadvantages of the selected method and the applicability to future analysis of PM. This study contributes to the understanding of the methods available for the monitoring of the composition of atmospheric particulate matter, thus providing insight into chemical environmental conditions and associated risks.

2. Methods

FTIR spectroscopy was selected to analyze samples collected in several different locations. In this work, a qualitative study of the selected method was conducted to assess the applicability towards future studies. The analysis of the field samples collected remained qualitative; however, these methods can be extended to include quantitative FTIR analytical techniques. Additionally, the nondestructive nature of the FTIR analysis allows for coupling with techniques such as GC-MS, ICP-MS, and XRF. A complete protocol for sample collection and analysis as developed in this study is presented in the appendix.

2.1 Sampling

PM samples were collected using a Sioutas cascade impactor with the Leland Legacy personal pump by SKC Inc. The Sioutas cascade impactor by SKC samples coarse, fine, and ultrafine particulate matter. One advantage of the Sioutas impactor is the ability to

simultaneously collect and partition $PM_{2.5}$ into five size ranges: $> 2.5 \mu\text{m}$, 1.0 to $2.5\mu\text{m}$, 0.50 to $1.0 \mu\text{m}$, $0.25\mu\text{m}$ to $0.50 \mu\text{m}$, and $< 0.25 \mu\text{m}$.

The Sioutas cascade impactor utilizes principles of inertia to separate particles of different sizes. The cascade impactor is composed of four impaction plates in series that serve as a surface for particle deposition. Figure 2.1 illustrates the typical design for a cascade impactor used in this study. Particles that enter the air stream will continue in a straight line when the flow direction changes significantly due to effects of inertia. Thus, larger particles will continue to the surface of the collection stage where they can adhere, while lighter particles are carried on to later stages. The width of the impaction slits above each plate is reduced as the air moves through the impactor. The reduction in slit width increases the velocity of the particles allowing smaller particles to be collected on the lower impaction stages.

PM samples were collected at 9 L/m for 24 hours on 4, 25mm , $0.5\mu\text{m}$ FALP (Teflon) filters, by Millipore, and one, 37mm , $2.0\mu\text{m}$ PTFE (Teflon) after-filter by SKC. Teflon filters gave the relatively cleanest IR absorbance spectrum. Additionally, Teflon has the benefit of minimizing particle bounce and preserving unstable compounds. Therefore, Teflon was chosen as a medium for particle collection. The analysis results for several filter types are presented in Figure 2.2.

To determine the effectiveness of the methods used, three samples were collected and analyzed. The first site was chosen as an indoor environment unaffected by smoking. The second field site was an alternate indoor location that is regularly subject to indoor cigarette smoke. An outdoor site was selected just outside the first smoke-free sampling site on a first story balcony. The outdoor sample was in contact with cigarette smoke originating in a community courtyard.

All three sites were located on the southern side of The Ohio State University just beyond university property. Table 2.1 describes the various sampling locations and existing conditions.

The same sample pump was operated for the duration of the 24-hour sampling period. The pump was calibrated to ensure performance within $\pm 5\%$ of 9 L/min prior to sampling. A self-regulation feature on the Leland Legacy pump automatically placed the pump on hold if this 5% limit were exceeded. All filters were handled with Teflon forceps and powder-free Teflon gloves at all times to avoid contamination. A method blank was handled exactly as each sample filter from pre-scan until the final analysis was completed. The method blank was carried in the field case during the course of sampling. During outdoor sampling, the equipment case was left outdoors by the particle collector for the duration of the 24-hour period.

Artifacts due to sampling are of concern in studies of this type (Turpin et al., 1994). The high flow rate of 9 L/min contributes to a large face velocity that could result in the volatilization of organic species. Further studies of this method must be conducted to ensure negligible sample loss. Inclusion of a downstream blank coated with an absorbent could be used to trap and measure any significant loss. Additionally, sample filters and the method blank can be spiked with a volatile organic prior to sampling. In this analysis, sampling artifacts were considered to be negligible due to the qualitative objectives of the experiment.

After completion of the 24-hour sampling phase, collection filters were removed and placed into 47 mm Petri Dishes. The case was then sealed with Teflon tape and frozen until completion of the analysis. Freezing samples immediately limits the amount of sample loss due to volatilization during storage. FTIR analysis of the collected samples was performed within 24-hours of sample collection. The effects of sample loss due to volatilization were studied by analyzing a single set of samples over a 72-hour period.

2.2 Fourier Transform Infrared (FTIR) Spectroscopy

FTIR Spectroscopy is used in this study to obtain qualitative bond and functional group information for PM samples. Quantification of identified functional groups in samples collected on Teflon filters can be performed using techniques as discussed by Krost and McClenney (1994). The non-destructive nature of FTIR additionally allows sample analysis by alternative techniques that were not explored in this particular study. This method protocol, however, was developed with consideration of possible future adaptation to include both quantification and coupled analytical techniques.

FTIR spectra were taken directly on the Teflon filters without sample preparation using a ThermoNicolet Avatar 370 E.S.P. FT-IR spectrometer. Both transmission and attenuated total reflectance (ATR) spectroscopy were used in this study for comparative purposes. The linear deposition pattern of PM on the filter surface favored the use of ATR spectroscopy; however, the high signal to noise ratio made it difficult to resolve the low concentrations of particles collected. For comparative purposes, one set of samples was analyzed using both ATR and transmission spectroscopy. A zinc selenide crystal was used for the ATR. Each spectrum was taken by averaging 200 scans at a resolution of 4 cm^{-1} . The spectra describe the absorbance of radiation as a function of wavenumber in the region of $4000 - 500\text{ cm}^{-1}$.

Prior to collection of sample spectra, the IR signal was maximized. An instrument blank was taken prior to each filter scan to account for differences in instrument response and atmospheric environment (i.e. H_2O and CO_2). A spectrum of each empty Teflon filter was taken prior to the collection of each sample. This spectra was saved to be used as a blank for the

collected PM sample. An FTIR spectrum of each filter was taken after the 24-hour collection period.

Subtraction of the blank (the spectrum of the empty Teflon filter) from the filter sample was performed for each sample. A sample spectrum of the blank Teflon filter is shown in Figure 2.3. Samples were placed in the filter holder in the same orientation and position for FTIR analysis before and after sample collection. Proper alignment insures that the asymmetric scattering from uneven stretch patterns of the Teflon is minimized, thus lowering the detection limits as suggested by Krost and McClenny (1994). A notch was cut in each filter prior to collection of the blank spectrum to aid with the proper alignment throughout the experiment. To determine the effect of alignment errors several spectra of a blank Teflon filter were taken at various arrangements.

The pre-scan filter blank and filter sample are shown in Figure 2.4. Removal of the blank spectrum from the sample was obtained through an interactive subtraction according to the following equation:

$$S = F - \beta I \quad (1)$$

where S is the sample spectrum, F is the final spectrum (i.e. sample + blank), I is the initial blank filter spectrum, and β is the spectral subtraction factor. A series of interactive subtractions was performed by varying the value of β . Changing the value of β allowed for identification of Teflon peaks within the sample spectrum. The height of Teflon peaks is dependent on the value of β , while actual sample absorbance remains fairly constant throughout the procedure. The optimal subtraction factor was chosen to minimize the Teflon peak at 554 cm^{-1} . This peak was

selected due to the consistency of both peak shape and height in all of the analyzed samples. The spectral subtraction factor, β , was determined to be approximately 1.0 for all samples.

Several spectral interferences were present in all of the samples. The Teflon absorbance from approximately $1250 - 1100 \text{ cm}^{-1}$ interferes with the sample spectrum. This distortion is a result of the spectral subtraction of Teflon absorbance bands. This region contains minor peaks for several functional groups as well as a major peak for sulfate. Selection of alternate peak locations suitable for qualitative analysis of the effected groups alleviated the interference problem (i.e. sulfate was characterized by the peak at 618 cm^{-1}). Additional interference from CO_2 is present in the region from $2300 - 2400 \text{ cm}^{-1}$; however, no peaks of interest to this study are found within this region.

Following the initial analysis of the PM samples, a differential washing procedure was performed to assess the polarity of the constituents. The sample filter was washed with increasingly polar solvents (i.e. hexane, dichloromethane, acetone, and water). The rinsing procedure used for each organic solvent was performed by placing the filter on a 3" büchner vacuum funnel and washing with 2 ml of solvent over a gentle vacuum flow. To perform a water rinse, 5 ml of water was let to stand on the face of the filter for five minutes and then removed. Each filter was then reanalyzed using FTIR spectroscopy after each rinse. Pre- and post-sample spectra and the sample blank were subtracted using Equation (1). This process allowed for the simplification of sample spectra and provided information on the polarity of the various collected PM fractions.

3. Discussion

Three sites were sampled for PM in five size fractions $> 2.5 \mu\text{m}$, $2.5 - 1.0 \mu\text{m}$, $1.0 - 0.5 \mu\text{m}$, $0.5 - 0.25 \mu\text{m}$, and $< 0.25 \mu\text{m}$. Multiple experiments were performed using the collected samples to assess the effectiveness of error reducing techniques, (i.e. filter alignment and sample loss over time). As a result, FTIR transmission spectroscopy was selected as the most appropriate technique for PM analysis on Teflon filters. Thus, all samples were analyzed using transmission FTIR to provide functional group information according to peak locations suggested by Maria et al. (2003). An example analysis of a PM sample is presented in Figure 3.1. Provided in Table 3.1 is a list of the peaks identified in this study. The peaks observed in all samples were typical of reported atmospheric PM composition.

3.1 Method Analysis

Several experiments were performed to insure the quality of the reported results. The aforementioned experiments included comparison of ATR and transmission FTIR, investigation of filter alignment on spectral analysis, and a study of sample loss over an extended amount of time. The results of these experiments were taken into consideration during the development of the sampling and analysis protocol.

As previously discussed both ATR and FTIR techniques have been used to study the composition of atmospheric PM. Figure 3.2 shows the spectrum of $\text{PM}_{0.5-0.25}$ collected at sampling site 3. In both the transmission and ATR spectrum similar spectral details are observed. However, the signal to noise ratio of the transmission spectrum is much greater than that for the

ATR. The better resolution of the transmission technique allows for a more accurate spectral subtraction and analysis. One example of the benefits of using transmission FTIR is the separation of the NO_3^- and CO_3^{2-} peaks (1462 and 1368 cm^{-1}) that is not observed in the ATR spectrum. As a result of this qualitative analysis, FTIR transmission spectroscopy has been selected for its ability to resolve less predominant features in the IR spectrum of PM samples.

The effect of filter alignment during acquisition of IR spectra has been suggested as a possible limit to the detection limits of the method (Krost and McClenny 1994). A blank Teflon filter was analyzed at multiple angles to investigate the effect of misalignment. The results of the experiment are shown in Figure 3.3. As the filter is rotated horizontally through 180°, the intensities of the Teflon absorbance vary. This effect could potentially interfere with the subtraction of the blank from the sample filter by varying the spectral subtraction factor β . This effect also contributes to increased interference in the 1250 – 1100 cm^{-1} region. To eliminate possible error from filter alignment, a notch was cut in each filter and properly aligned with a marker on the filter holder throughout the experiment.

To study the effect of sample loss and potential contamination during storage sample 1 was studied over a period of 72 hours. Figure 3.4 shows the results of this analysis performed on two separate PM fractions. According to the developed protocol, analysis of the collected samples was conducted 24 hours after sample collection. The graph of both $\text{PM}_{1.0-0.50}$ and $\text{PM}_{2.5-1.0}$ display the initial spectrum, labeled 24 hours, and two additional analyses performed over the next 48 hours. In the analysis the $\text{PM}_{2.5-1.0}$, a decrease in the peaks observed in the 1000 cm^{-1} region and in the 2900 cm^{-1} C-H stretching region with time is observed. This reduction in peak intensities over the 72-hour period indicates significant sample loss. Conversely, the same absorbance regions in the $\text{PM}_{1.0-0.50}$ samples are increased over the 72-hour period. Thus a

source of contamination was encountered after the initial sample spectrum was collected. To minimize the risk of sample loss and contamination, it is suggested that an initial spectrum of the sample filters be collected immediately after the 24-hour sampling period is complete.

3.2 Sample Results

Particulate samples of the following PM fractions $> 2.5 \mu\text{m}$, $2.5 - 1.0 \mu\text{m}$, $1.0 - 0.50 \mu\text{m}$, $0.50 - 0.25 \mu\text{m}$, and $< 2.5 \mu\text{m}$ were collected at three locations. Using absorbance ranges suggested by Maria et al. (2003), several functional groups were successfully identified in all of the samples collected. The identified functional groups (i.e. NO_2^- , $\text{C}=\text{O}$, NH_4^+ , etc.) were typical of the expected composition of the PM samples collected. Further analysis of the filter samples revealed additional information about the chemical composition of the PM samples as well as the usefulness of the developed measurement technique.

The ability of the particle sampler to separate PM fractions can be validated by looking at the IR spectrum of the collected filter samples at a given location. Figure 3.5 presents a plot of the five PM fractions collected at sampling site 2. It can be observed that the intensities of functional group absorbance varies with particle size. This can be attributed to the concentration of particle density in the fine PM fractions. The observation in the fine PM fractions of high concentrations of NH_4^+ (1462 cm^{-1}), sulfates (616 cm^{-1}), and polar organics (2958 , 2917 , 2849 , and 3076 cm^{-1}) that are removed in the hexane solvent wash agree the expected composition of fine particulates. In addition, the large absorbances in the fine PM fractions can be attributed to

the high concentration of number density in the lower size fractions leading to more efficient particle loading during sample collection.

Samples 1 and 2 are indoors area samples collected in both a smoke-impacted environment and a smoke-free atmosphere and sample 3 was collected at an outdoor location (see Table 2). Figure 3.6 shows the spectrum of $PM_{2.5-1.0}$ collected at all three locations. This fraction contains particles resulting from mechanical processes (i.e. soils, sea salts, dust, etc.) Absorption intensities in the sample collected outdoors are significantly higher than those in samples 1 and 2. This suggests that the concentrations of large particles at an outdoors location are larger than the amount observed indoor. This observation is consistent with all general literature published on the subject of indoor PM concentrations. The coarse fraction shown is removed by natural defense mechanisms of our respiratory system. Thus the high levels observed at the outdoor location do not pose a significant threat to human health.

Figure 3.7 shows $PM_{0.50-0.25}$ collected at all three locations. Contrary to the results observed in the $PM_{2.5-1.0}$ fraction, the indoor smoking sampling site contains significantly greater amounts of PM. The bottom two spectra, indoors non-smoking and outdoor, both show marginally equivalent levels of PM. The particles sampled in the range of 0.50 to 0.25 μm are able to enter the gas exchange regions of our lungs. Thus, the significantly higher levels of $PM_{0.50-0.25}$ observed at an indoor smoke impacted environment indicate the possibility for increased chance of negative health impacts. This observation is consistent with current research on the impacts of cigarette smoking. For additional information on the chemical composition of this fraction a differential solvent wash was performed.

After the initial FTIR analysis, $PM_{0.50-0.25}$ collected at location 2 was sequentially rinsed in hexane, dichloromethane (DCM), acetone, and water. FTIR was performed after each solvent

rinse. The resulting spectra are presented in Figure 3.8. Shown is the initial sample spectrum, the hexane-rinsed filter sample, the DCM rinsed sample, the acetone rinsed sample, and the water rinsed filter sample. Hexane removed non-polar organic compounds; DCM removed both non-polar and some polar organics; acetone removed polar organic compounds and water removed the very polar organic compounds remaining and inorganic salts (i.e. NH_4^+) from the filter sample. Teflon absorbance can be observed in the region of $1250 - 1100 \text{ cm}^{-1}$ that interferes with surrounding peaks.

The sample spectrum before the differential solvent washes contains strong C-H stretching absorbances ($2958, 2917, 2849, \text{ and } 3076 \text{ cm}^{-1}$). The hexane rinse radically reduced these absorbances indicating low polarity organic compounds. The absorbance observed at 3067 cm^{-1} is typical of aromatic C-H absorbance. Such absorbance are characteristic of PAHs emitted in cigarette smoke (Hoffmann and Hoffmann 1997). Most of the carbonyl ($\text{C} = \text{O}$) peak at 1642 cm^{-1} is removed in the hexane wash suggesting low polarity carbonyl containing compounds. Examples of low polarity carbonyl compounds are surfactants such as those found in the gas exchange regions of our lungs.

According to Hoffmann and Hoffmann (1997), carboxylic acids ($1711 \text{ cm}^{-1} \text{ C} = \text{O}$) and quinones ($1650 \text{ cm}^{-1} \text{ C} = \text{O}$) are major components in cigarette smoke. These groups are observed as part of the broad carbonyl absorption band from $1600 - 1800 \text{ cm}^{-1}$ a majority of which is removed in the first hexane wash. A component of this $\text{C} = \text{O}$ absorption band grows after the final water wash, with respect to the DCM wash. This effect is possibly due to the ineffectiveness of the water to remove the entire carbonyl fraction. This results from water's inability to penetrate the non-polar surface of the Teflon filters. The absence of dominant $\text{C} = \text{O}$ bands in sample 1 is consistent with the absence of cigarette smoke at the sampling location.

The sample shown in Figure 3.7 represents the composition of fine particulate matter. This fraction has the ability to penetrate deep within the cardiorespiratory system into the gas exchange regions of the lungs. From there PM has the ability to directly enter the blood stream and cause significant damage within the human circulatory system. The carcinogens observed in cigarette smoke (i.e. carboxylic acids, quinones, and large PAHs) are particularly dangerous due their corrosive nature. The high concentrations of these observed in the Hexane wash confirm general fears about the harmful nature of cigarette smoke inhalation.

4. Conclusions

Characterization of human exposure to air-toxics can increase our ability to identify sources of PM as well determine solutions to prevent negative health related effects. Additionally, the analysis of the composition of particulate matter remains important to the investigation of chemical environmental conditions specific to the atmosphere. The addition of more efficient and cost effective techniques of PM analysis increases our ability to intensively monitor local air quality.

The selected methods of PM collection and analysis have proven to be an effective and inexpensive method. PM samples collected were fully characterized without sample preparation time. The resulting information collected from sample analysis provided insight into the chemical environment of the various PM size fractions. This qualitative data is important for the estimation of the properties of PM, especially as it pertains to its interaction with the human

body. Additionally the nondestructive nature of the method has left room for method extension to include methods such as GC, GC-MS, ICP-MS, or XRF.

The method as presented is sufficient to provide a general picture of the chemical environment of atmospheric PM. However, the utilization of quantitative methods of analysis would be beneficial to further understanding the nature of PM. FTIR absorbivities (peak area per micromole of functional group) of the identified functional groups varies significantly. As an example, the absorbivity of C = O is 0.061 while that of C-H is 1.04. Thus a C = O peak which is qualitatively 1.7 times that of a C-H peak represents roughly the same concentration of functional group. Therefore it is necessary to perform a quantitative analysis to assess the composition of PM samples as it relates to relative levels of components within a single size fraction. However, it remains useful to qualitatively compare functional group concentration in separate PM samples.

Although the sample mass collected using the Sioutas impactor was relatively small, this experiment has the ability of the developed method to analyze atmospheric PM. Using the samples described above, IR spectral features characteristic of smoke-impacted environments have been distinguished from those of smoke-free environments. Expected variations in size dependant PM composition have also been validated by the analysis of the various size fractions sampled. This qualitative analysis of the selected method has demonstrated its ability to be use in future studies. Further work to expand these methods to include quantitative analysis will enhance its applicability towards additional field studies of atmospheric PM.

5. Appendix

FTIR Analysis of Aerosol Samples Collected on Teflon Filters

Purpose: To collect and analyze particulate matter samples using FTIR spectroscopy.

Inventory:

Sioutas Impactor by SKC
Leland Legacy Pump by SKC
2" Rubber pump tubing
1.0 micron, 25mm FALP filters by Millipore (5)
2.0micron, 37mm PTFE Filters by SKC (2)
Teflon forceps
Petri Dishes (7)
Powder free vinyl gloves
Teflon Tape

Sioutas Impactor preparation:

1. Prior to filter loading, disassemble filter cartridge and remove o-rings and plastic filter retainers. To remove o-rings insert head of a flat-head screwdriver into the notch in the inner wall of the plate. Gently lift ring up and out.
2. Wash the filter stages and housing unit using a warm soap-water solution.
3. Thoroughly dry the components using compressed air.
4. Check impaction slits to ensure that no debris is blocking passage (*Do not insert objects into impaction slits to remove obstructions*).

Leland Legacy pump preparation:

**Charge Legacy Pump at least 24 hours prior to sampling*

1. Turn the pump on by pressing any key.
2. Enter the navigation menu by pressing [** Δ∇ **] in sequence and "SETUP" will appear on display.

3. To scroll through setup parameters press * key, parameters will repeat after LCD shows “END”
4. Set flow to 9 L/min
5. Set calibration to 0.00*
6. Sampling time varies upon experiment, for 24-hour collection time enter 1440 min.
7. Press [$\Delta\nabla$] simultaneously when LCD reads, “END” to exit setup, pump will be in hold.
8. To begin sampling and to start pump, press [$\Delta\nabla$] simultaneously while not in setup menu. Prior to sampling the pump must be run at 9 L/min to ensure a stable flow.
9. To clear settings after sample collection enter setup menu, see step 2, press * until “Clr” appears then press
[$\Delta\nabla$], all settings will be cleared to factory settings.
10. To turn pump off hold * key until count down appears on LCD.

* The pump is calibrated to run at $\pm 5\%$ of the indicated flow rate. If this is exceeded the following symbol will appear and the pump will be placed on hold: $\Sigma\Rightarrow$ Calibrating the pump using a recommended calibrator will ensure correct flow rate with sampler attached. Since no calibrator was used in this experiment error of 5% was assumed on desired flow. When attaching sampler to pump adjust the tightness of thumbnuts to functional range. If thumbnuts are too tight the pump will overload and 5% error range will exceed. Trial and error is required to find the proper tightening without a pump calibrator.

Sample Preparation:

1. Prior to collection of filter spectra, cut a notch in the outer edge of the filter. Be sure not to place incision within the expected line of sample deposition. This will serve as an alignment marker to ensure correct positioning in filter holder during spectra collection.
2. Place filter into filter holder and record alignment of the filter according to the positioning of the notch made in step 1.
3. Collect background spectra on Avatar 370 Nicolet FTIR spectrometer by Thermo Nicolet using 200 scans at a resolution of 4 cm^{-1} .
4. Collect sample spectra of a clean 25 mm FALP Millipore filter and subtract background spectra taken during step one. Designing an experiment using Omnic software will help to perform this step automatically. Use the following steps to design a collection experiment.
 - a. In the toolbar menu click on 'collect'. Then choose 'Experiment setup...' and enter the appropriate number of scans and resolution (200 and 4 cm^{-1} respectively).
 - b. Select option in 'Background handling' box to perform a background scan prior to each sample.
 - c. Choose save option and name experiment accordingly.
 - d. Follow step 1 and 2 and respond to the prompts for background and sample spectrum collection.
4. Save filter pre-scan for later use as a background for collected sample.

5. Place sample filter in a Petri dish labeled for the corresponding collector stage and date. (For example: label filter “A_041505” and use in stage A during sample collection).
6. Repeat the above steps for 5, 25mm Millipore filters and 2, 37mm SKC filters representing stages A, B, C, D and the after filter as well as two method blanks for each filter type.

Sample Collection assembly:

1. Remove compression ring from outer plate and insert 37mm after-filter between spacer ring and compression ring.
2. Place a collector plate into top of outer plate ensuring that the external alignment marks are correctly oriented.
3. Use Teflon forceps to place a 25 mm filter onto the filter stage of the collector plate and place a filter retainer on top of the filter. Press down with forceps to attain a tight fit.
4. Place accelerator plate “D” on top of the collector plate ensuring correct alignment of outer-marks.
5. Repeat steps 2-4 for stages C-A alternating collector plate and accelerator plate.
6. Slide inlet plate into place on threaded studs and finger tighten thumbnuts. (See comment on Pump preparation for additional information regarding thumbnut tightening).
7. Attach rubber tubing to outlet plate of Sioutas sampler and to the inlet of Legacy pump.
8. When ready to begin sampling turn on pump as explained in step 8 of pump preparation section.
9. Adjust thumbnuts as necessary to ensure flow rate within 5% of desired rate. (See step 6)

Sample Storage:

1. Disassemble sampler being careful not to invert filters.
2. Remove filters using forceps and place into labeled Petri dishes according to stage name and date.
3. If analysis is to be performed at a later date seal Petri dishes with Teflon tape and place into a freezer until analysis.

Sample Analysis:

1. Using the Omnic program, open saved experiment. (Use 200 scans at 4 cm^{-1})
2. Collect a background spectra followed by spectrum of filter sample, and subtract background from sample. As explained above, possibly automated if included in experimental design.
3. Save filter sample spectra.
4. Place filter in corresponding Petri dish and return to freezer until required in the future.
5. Repeat steps 2-4 for the remaining 6 filters.
6. While operating the Omnic program, open a pair of filter pre-scan and post-scan spectrum in the same window as shown in Figure 2.4.
7. Select both graphs using ctrl+w or select all from the edit menu.
8. Choose subtract* option from the toolbar displayed above the window.
9. Switch the positioning of the graphs to ensure subtraction of the pre-scan from the post-scan.
10. Adjust the scaling factor on the left side of the window manually to minimize the peak observed at 554 cm^{-1} as a result of Teflon absorbance. Figure 5.1 shows the peak at 554 cm^{-1} .

11. Save the resulting spectra as the sample spectra.

* Subtraction of the spectra is obtained using the following equation:

$$S = F - \beta I$$

Where S is the sample spectrum derived from subtracting the blank filter spectrum (I) from the final spectrum F (sample plus blank filter spectrum) using the spectral subtraction factor 'β' determined from a series of subtractions at various values (distinguishes Teflon peaks from sample).

Differential Washing Procedure:

1. After collection of initial sample spectrum, place the filter sample into a 3" büchner vacuum funnel connected to a low vacuum flow.
2. Slowly rinse the face of the filter sample with 2 ml of spectral grade Hexane allowing solvent to pass through the filter.
3. Let the filter dry completely then remove from vacuum suction.
4. Reanalyze filter sample using FTIR and save spectrum for analysis as previously explained.
5. Repeat steps 1 – 4, 2 times using spectral grade acetone and dichloromethane.
6. Place filter on a clean surface and add 5 ml of nanopure water to the face of the filter completely covering the sample collected.
7. Let the water sit on the filter for 5 minutes and then pour off. Wait an additional 5 minutes or until the filter is completely dry and reanalyze using FTIR.
8. Save final spectra for spectral subtraction and analysis.

5. Figures and Tables

Table 1.1. 50% cutoff Points and Approximate Range of Particle Diameters Collected in a Four-Stage Impactor.

Stage	50% Cutoff Point (μm)	Approximate range of diameters captured by each Stage (μm)	ΔD (μm)
1	8.0	14.0 – 6.0	8.0
2	4.0	6.0 – 2.8	3.2
3	1.5	2.8 – 1.0	1.8
4	0.5	1.0 – 0.3	0.7
After-filter	< 0.5	0.3 – 0.001	0.3

Adapted from Pitts and Pitts 1999

Fig. 1.2 Infrared beam passing through an ATR crystal.

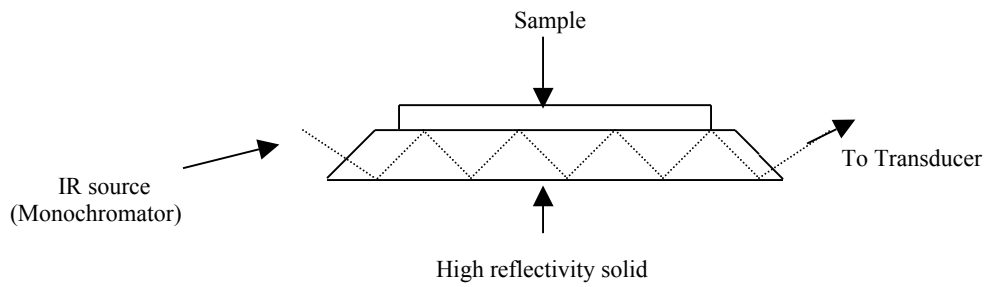
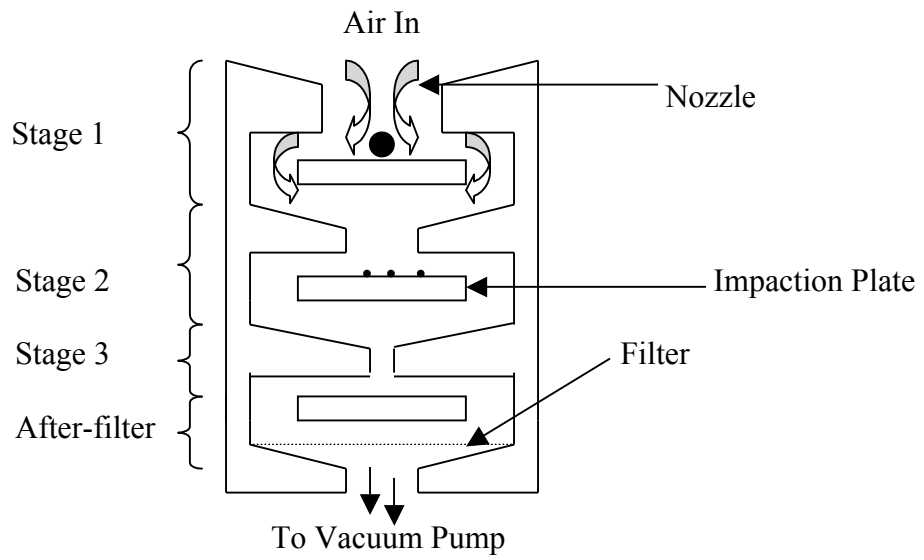


Fig. 2.1. Example of a cascade impactor representative of the Sioutas impactor.



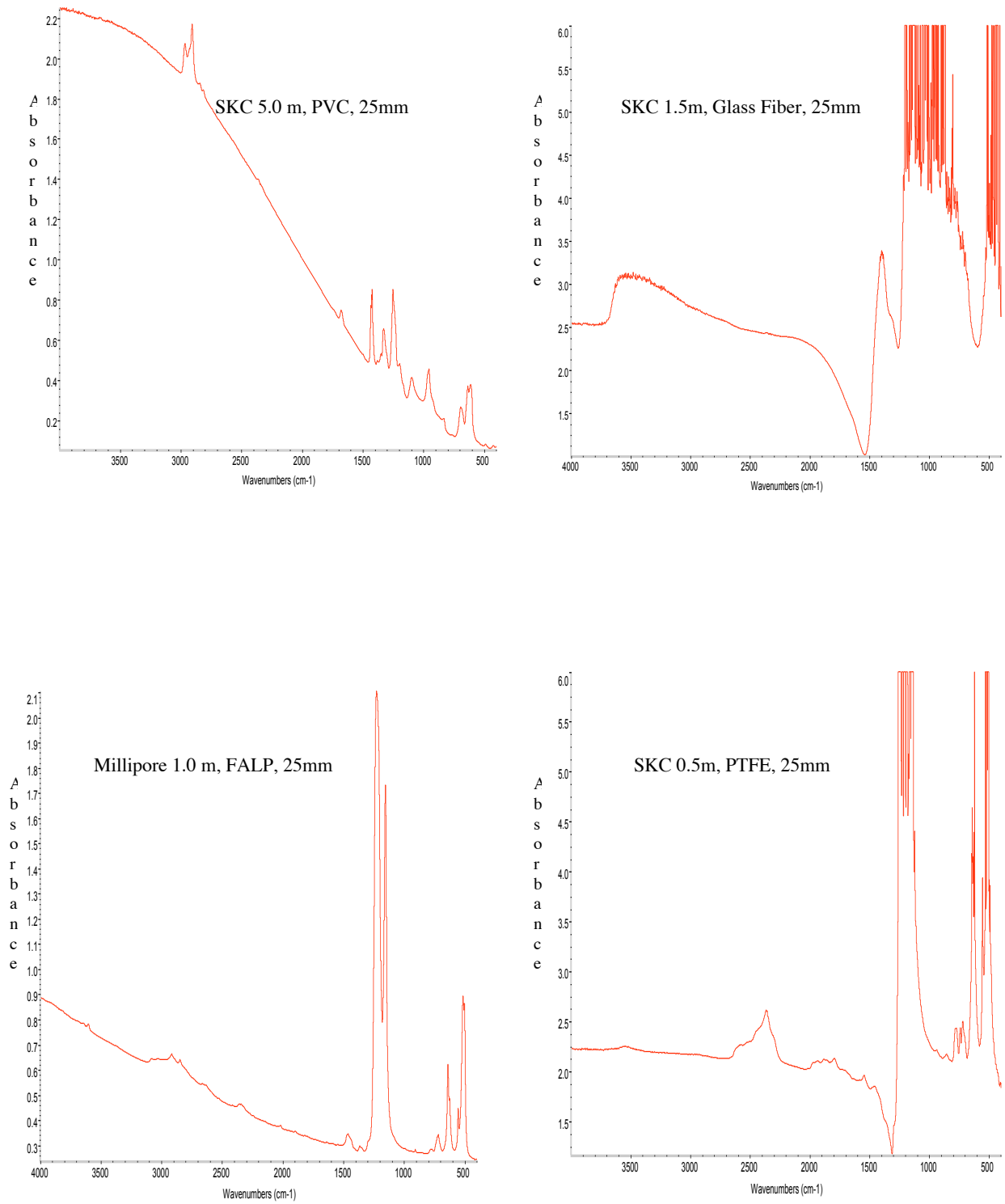


Fig. 2.2. Absorbance spectra of the four filter types considered as a surface for sample collection and analysis.

Table 2.1. Three particulate matter samples collected to demonstrate analytical techniques utilized.

Sample	Location	Analytical Methods	Date of Collection
1	Indoor Non-smoking	Transmission FTIR	05.09.05
2	Indoor Smoking	Transmission, ATR FTIR	05.16.05
3	Outdoor	Transmission FTIR	05.11.05

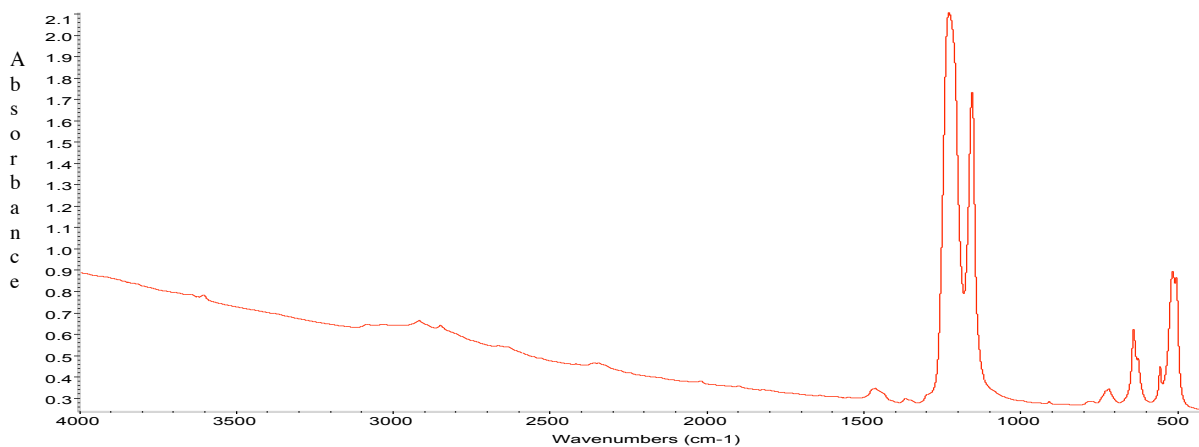


Fig. 2.3. Typical blank spectrum of a Teflon filter by Millipore. Peaks at 1213 and 1152 cm^{-1} interfere with peak identification in this region.

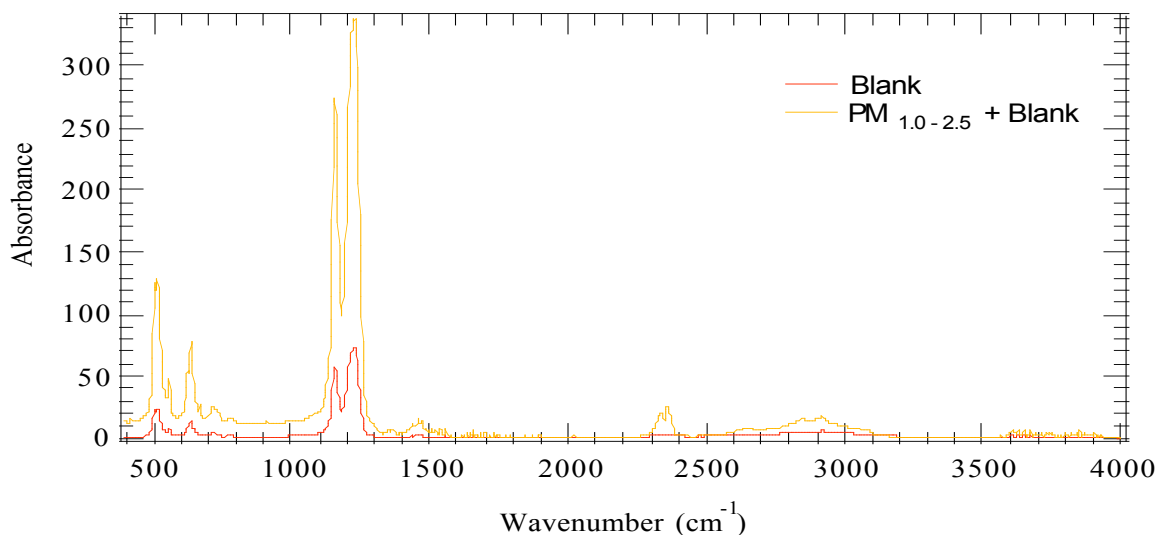


Fig. 2.4. Comparison of the filter blank and filter sample 1 taken on 05.09.05.

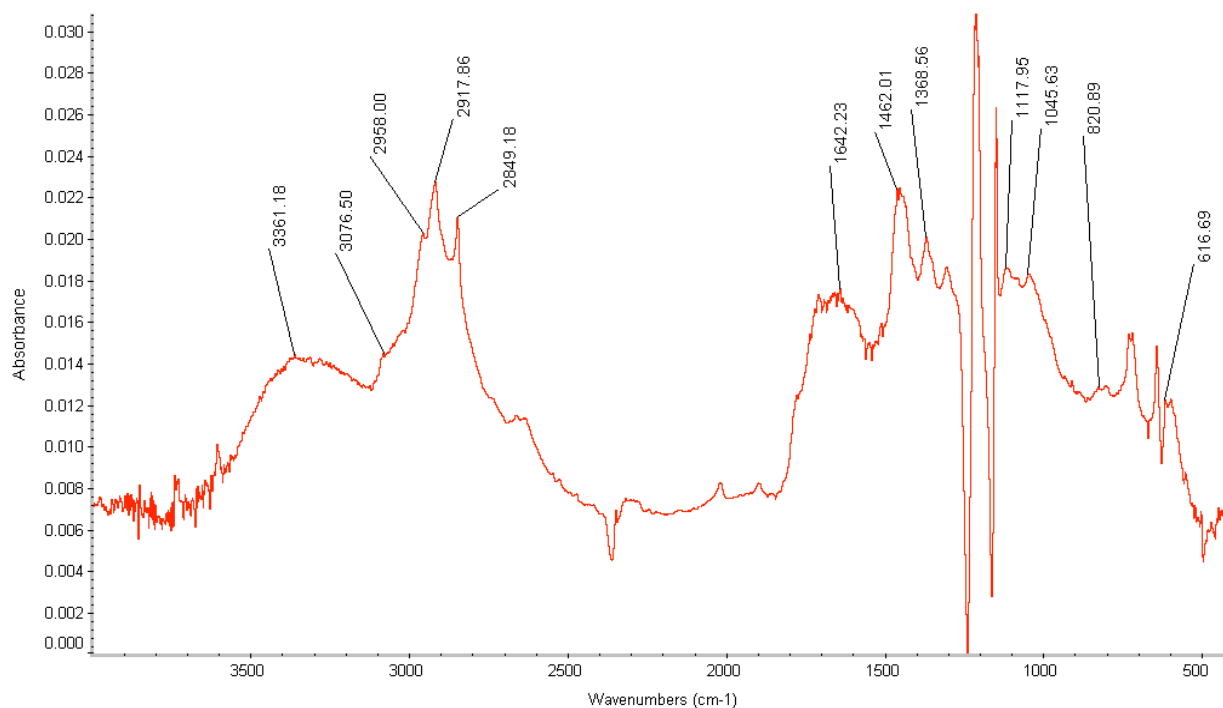


Fig. 3.1. Spectrum of $PM_{0.50-0.25}$, taken indoor at location 2. The peaks marked were assigned as follows (from left to right) SO_4^{2-} (616 cm^{-1}), NO_3^- (820 cm^{-1}), SiO_4^{4-} (1045 cm^{-1}), NO_3^- (1368 cm^{-1}), CO_3^{2-} and NH_4^+ (1462 cm^{-1}), $C=O$ (1642 cm^{-1}), $C-H$ aliphatic (2849 and 2917 cm^{-1}), $C=CH$ alkene (2958 cm^{-1}), $C=CH$ aromatic (3076 cm^{-1}), and $C-OH$ (3361 cm^{-1}).

Quantified (cm ⁻¹)	Functional Groups	Name
3100-3500	C-OH	Alcohols
3000-3100	C=C-H	Aromatic carbon
2900-3100	C=C-H	Alkene carbon
1452-5, 2800-3000	C-H	Aliphatic carbon
1640-1850	C=O	Carbonyl
1630	C-NH2	Amines
1410-35, 3030-52, 3170-3200	NH ₄ ⁺	Ammonium
860-80, 1410-90	CO ₃ ²⁻	Carbonate
815-40, 1350-80	NO ₃ ⁻	Nitrate
772-812, 1035	SiO ₄ ⁴⁻	Silicate
612-5, 1103-35	SO ₄ ²⁻	Sulfate

Table 3.1. Peaks used in FTIR qualitative study of aerosol functional groups, adapted from Maria et al. 2003.

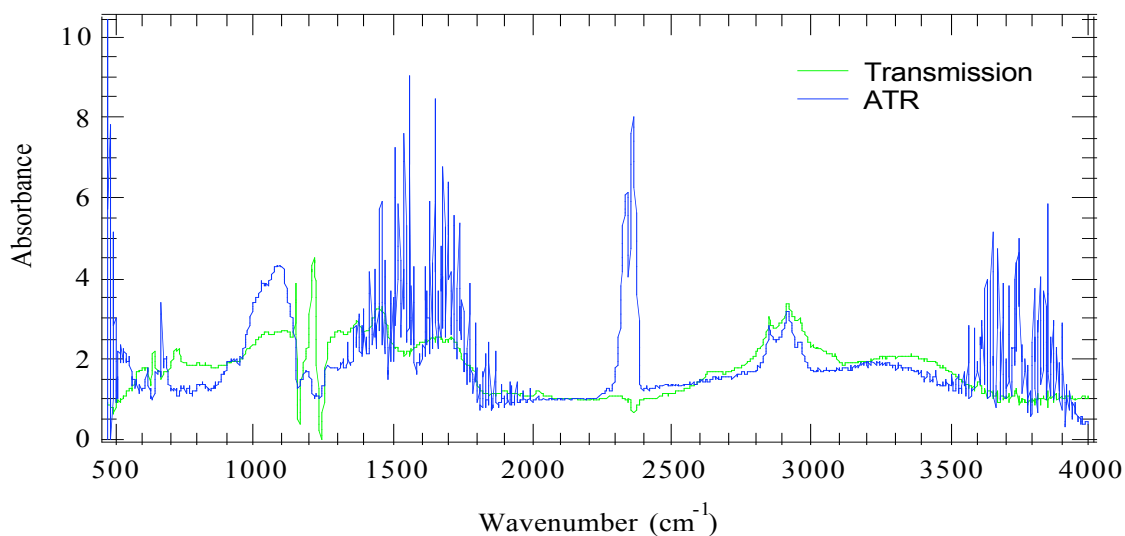


Fig. 3.2. Comparison of transmission and ATR-FTIR analytical techniques. The above figure depicts the spectra of PM_{0.5-0.25} collected at sampling site 3.

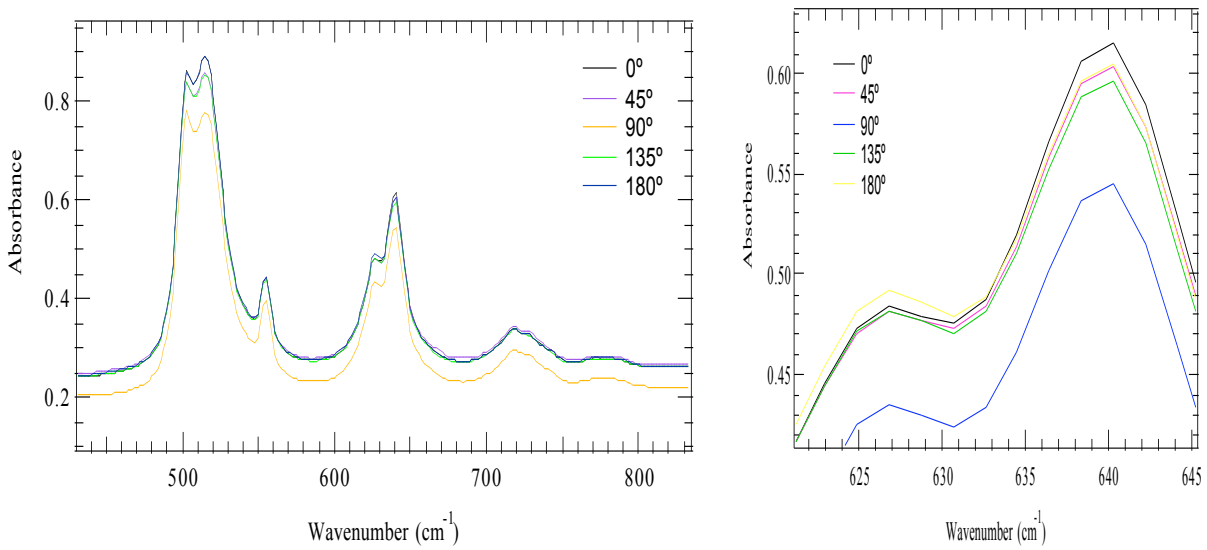


Fig 3.3. Absorbance spectra of a blank Teflon filter at various alignments during acquisition. The graph to the right shows a more detailed picture of the highlighted region of Teflon absorbance.

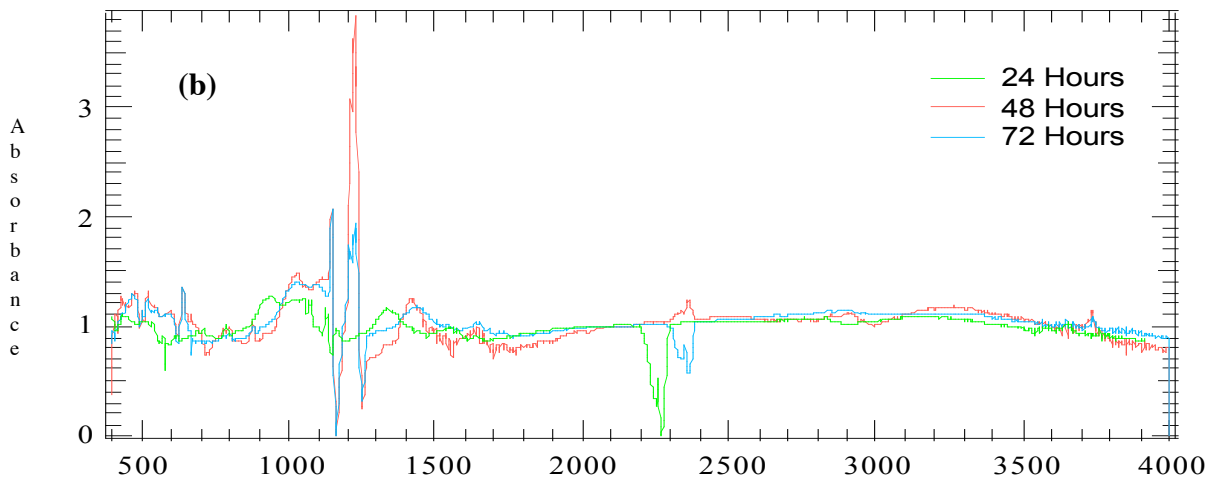
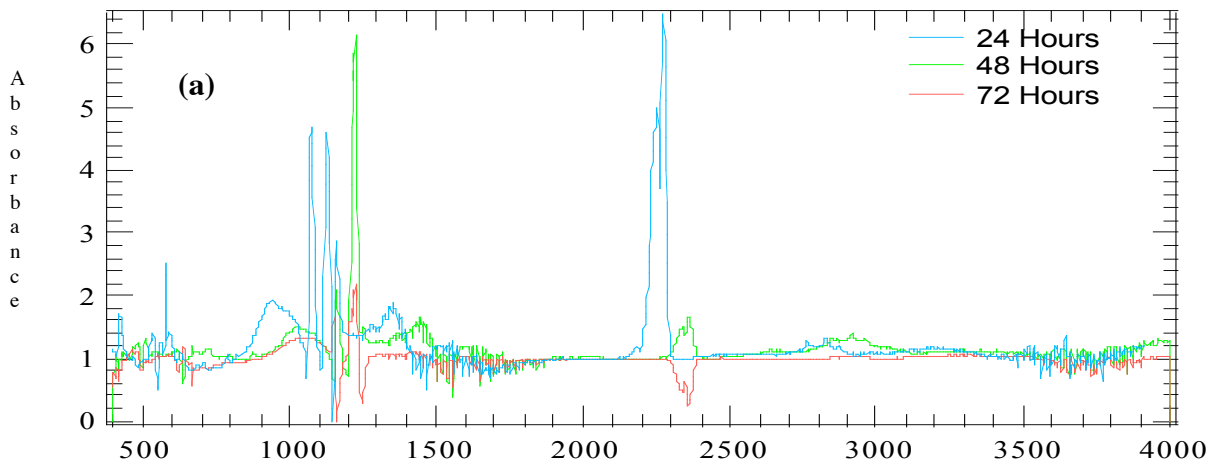


Fig. 3.4. (a) $PM_{1.0-0.50}$ sample from site 1 analyzed over a 72-hour period; (b) $PM_{2.5-1.0}$ sampled at site 1 analyzed over a 72-hour period.

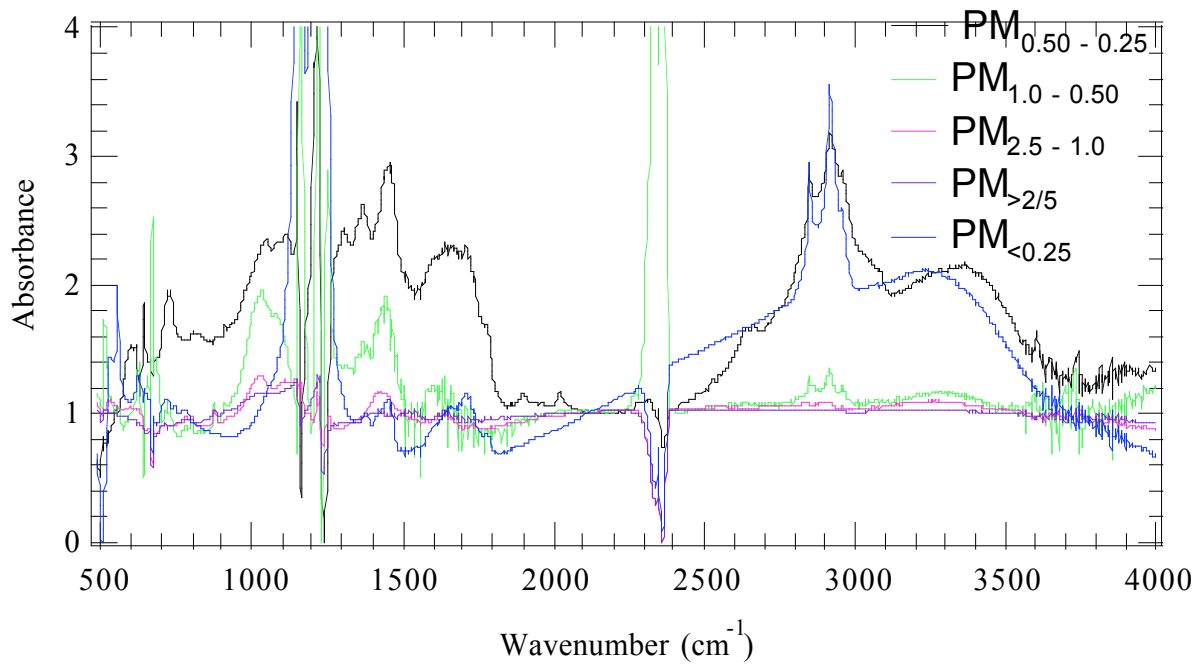


Fig. 3.5. Comparison of five PM fractions collected and separated by the Sioutas inhaler. This sample was collected at site 2 on 05.16.05.

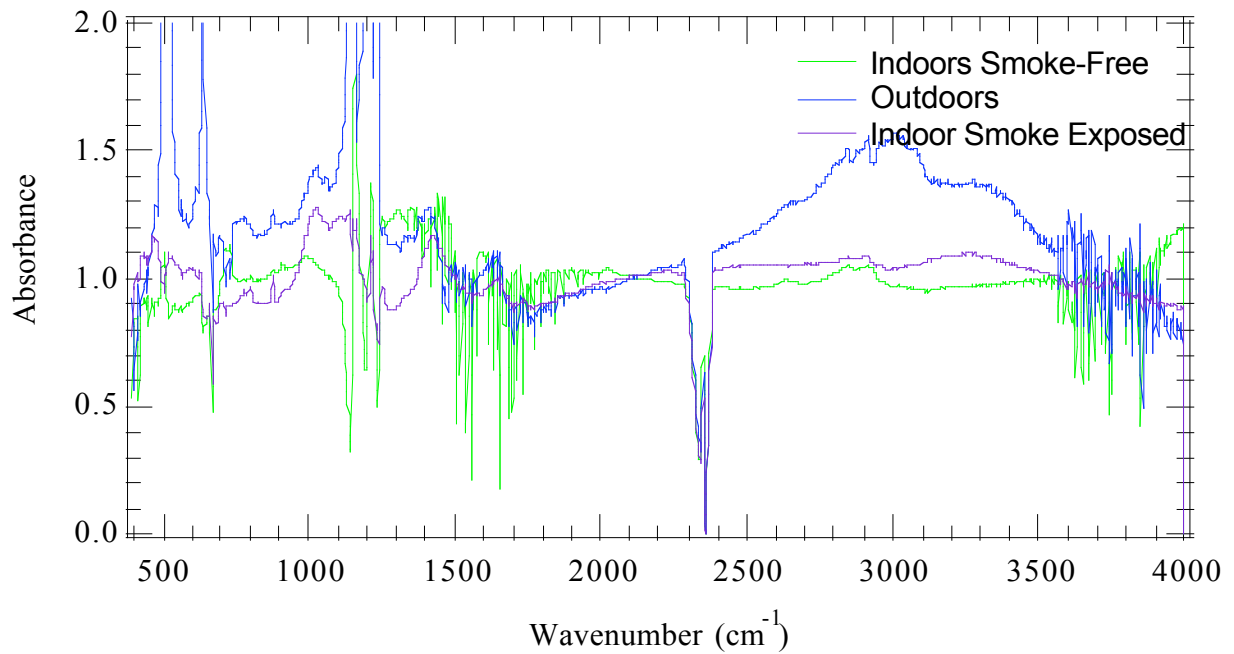


Fig. 3.6. Spectrum of PM_{2.5-1.0} collected at all three sampling locations.

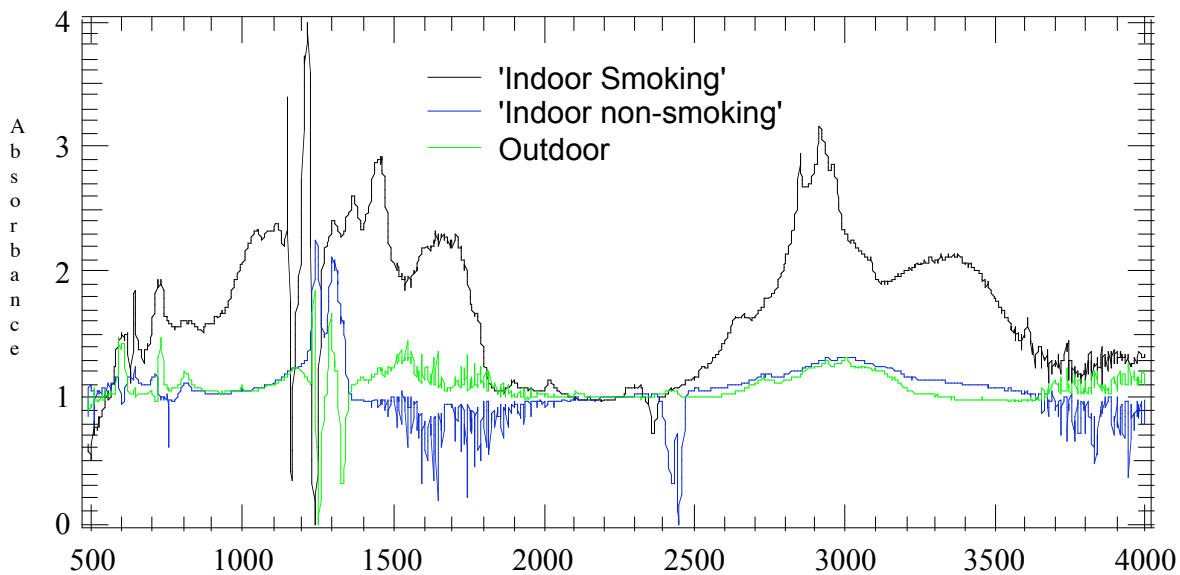


Fig. 3.7. Spectrum of PM_{0.50-0.25} collected at all three sampling locations.

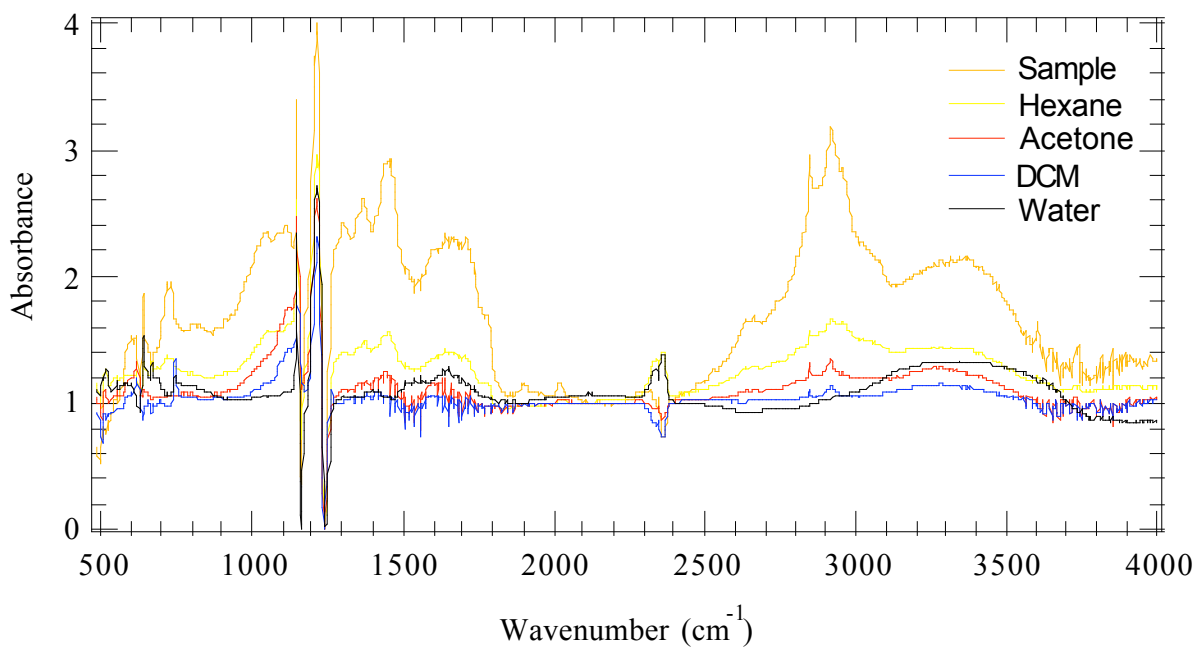


Fig. 3.8. FTIR spectrum of PM_{0.50-0.25} collected at site 2, an indoor smoke-impacted residence. Sequential rinses were performed to obtain information on aerosol polarity. Solvents used in sequential order were hexane, acetone, dichloromethane (DCM), and water.

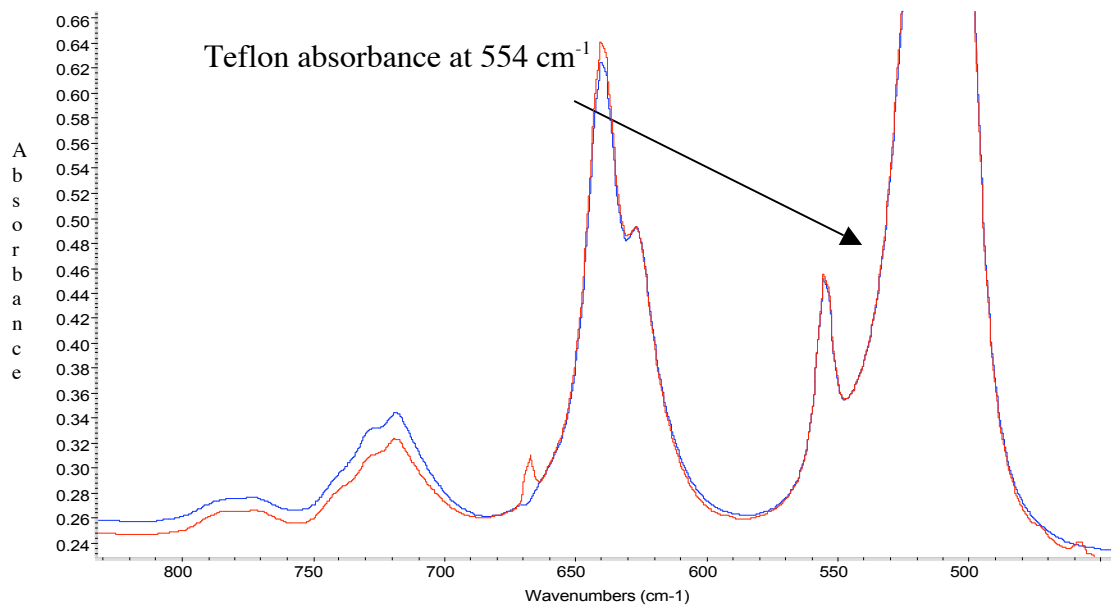


Fig. 5.1. Identification of the Teflon peak at 554 cm^{-1} . This peak is used to determine the correct scaling factor for subtraction of filter pre-scans from post-scans.

References

Blando, J.D., Porjca, R.J., Li, T., Bowman, D., Liyo, P. and Turpin, B.J. (1998) Secondary Formation and the Smoky Mountain Organic Aerosol: An Examination of Aerosol Polarity and Functional Group Composition During SEAVS. *Environmental Science and Technology* 32, 604 – 613.

Braga, A.L.F., Zanobetti, A., and Schwartz, J. (2001), “The lag structure between particulate air pollution and respiratory and cardiovascular deaths in ten U.S. cities,” *Journal of Occupation and Environmental Medicine*, 43, 927-933.

Dockery, D.W. and Spengler, J.D. (1981). Personal Exposure to Respirable Particulate and Sulfates, *J. Air Pollution. Control Association* 31:153-159.

Finlayson-Pitts, B.J, Pitts, J.J., 1999. Chemistry of the Upper and Lower Atmosphere. *Academic Press*, San Diego.

Heok, G., Brunekreef, B., Fischer, P., and Van Wijnen, J. (2001), “The association between air pollution and heart failure, arrhythmia, embolism, thrombosis, and other cardiovascular causes of death in a time series study,” *Epidemiology*, 12, 355-357.

Hoffmann, D., and Hoffmann, I. (1997). The Changing Cigarette, 1950 – 1995, *Toxic Environmental Health* 50: 307 – 364.

Jacobson, M.C., Hansson, H.C., Noone, K.J., Charlson, R.J., 2000. Organic atmospheric aerosols: review and state of the science. *Reviews of Geophysics* 38, 267-294.

Krost, K.J., and McClenney, W.A. (1994). FT-IR Transmissions Spectroscopy for Quantification of Ammonium Bisulfate in Fine-Particulate Matter Collected on Teflon[®] Filters., *Applied Spectroscopy* 48: 702 – 705.

Lin, M., Chen, Y., Burnett, R. T., Villeneuve, P.J., and Krewski, D. (2002), “The Influence of Ambient Coarse Particulate Matter on Asthma Hospitalization in Children,” *Environmental Health Perspectives*, 110. 575-581

Maria, S.F., Russel, L.M., Turpin, B.L., Porcja, R.J., 2002. FTIR measurements of functional groups and organic mass in aerosol samples over the Caribbean. *Atmospheric Environment* 36, 5185 – 5196.)

Maria, S.F., Russel, L.M., Turpin, B.J., Porcja, R.J., Campos, T.L., Weber, R.J., and Huebert, B.J. (2003). Source signatures of carbon monoxide and organic functional groups in Asian Pacific Regional Aerosol Characterization Experiment (ACE-Asia) submicron aerosol types. *Journal of Geophysical Research*, Vol. 108, No. D23, 8637.

Marley, N., Gafney, J.S., Cunningham, M.M., 1993. Aqueous greenhouse species in clouds, fogs, and aerosols. *Environmental Science and Technology* 27, 2864-2869)

Shaka, H. and Saliba, N. (2004). Concentration measurements and chemical composition of PM10-2.5 and PM2.5 at a coastal site in Beirut, Lebanon. *Atmospheric Environment* 38, 523 – 531.

Turpin, B.J., Heringm S.V., and Huntzicker, J.J., (1994). Investigation of Organic Aerosol Sampling Artifacts in the Los Angeles Basin, *Atmospheric Environment* 28:3061-3071.